Journal of Applied Electrochemistry **34**: 323–330, 2004.

Electrode reaction of the Np^{3+}/Np couple at liquid Cd and Bi electrodes in LiCl–KCl eutectic melts

O. SHIRAI[1,*,†], K. UOZUMI[2], T. IWAI[1] and Y. ARAI[1]
[1]*Department of Nuclear Energy System, Japan Atomic Energy Research Institute, Oarai-machi, Higashiibaraki-gun, Ibaraki-ken, 311-1394 Japan*
[2]*Pyro-Process Fuel Cycle Project, Central Research Institute of Electric Power Industry, 2-11-1, Iwado Kita, Komae-shi, Tokyo, 201-8511 Japan*
*(*author for correspondence: shirai@popsvr.tokai.jaeri.go.jp)*
[†]*Present address: Research Reactor Institute, Kyoto University, 2-1010, Asashiro Nishi, Kumatori-cho, Sennan-gun, Osaka 590-0494, Japan; e-mail: shirai@HL.rri.kyoto-u.ac.jp*

Received 13 December 2002; accepted in revised form 4 October 2003

Key words: alloy formation, bismuth, cadmium, cyclic voltammetry, LiCl–KCl eutectic salt, molybdenum, neptunium

Abstract

The electrode reactions of the Np^{3+}/Np couple at liquid Cd and Bi electrodes were investigated by cyclic voltammetry at 723, 773 and 823 K in the LiCl–KCl eutectic melt. It was found that the diffusion of Np^{3+} in the salt phase was the rate-determining step in the cathodic reaction when the concentration of $NpCl_3$ was less than about 1 wt % and the liquid Cd or Bi phase was not saturated with Np. The redox potentials of the Np^{3+}/Np couple at the liquid Cd electrode at 723, 773 and 823 K were observed to be more positive than those at the Mo electrode by 0.158, 0.140 and 0.126 V, respectively. The potential shift results from a lowering of the activity of Np in the Cd phase according to the formation of the $NpCd_{11}$ alloy at 723 K and $NpCd_6$ at 773 and 823 K. The redox potentials of the Np^{3+}/Np couple at the liquid Bi electrode at 723, 773 and 823 K were more positive than those at the Mo electrode by 0.427, 0.419 and 0.410 V, respectively, which is attributable to a lowering of the activity of Np in the Bi phase due to the formation of $NpBi_2$.

1. Introduction

Pyrochemical reprocessing of nuclear fuels using molten salts has been developed for recovering actinides from spent metallic and nitride fuels [1–5]. In the electrorefining step of the pyrochemical reprocessing, spent metallic or nitride fuels are dissolved at the anode in a LiCl–KCl eutectic melt, and the actinide elements are recovered as metals at the cathode. It has been proposed that U is selectively recovered at the solid cathode, since the formation energy of UCl_3 is lower than those of the chlorides of other actinides. Pu and the minor actinides (MAs) are then obtained at the liquid metal cathode as a mixture of U, Pu and MAs, due to their low activity coefficients in the liquid metals such as Cd, Bi etc. [2, 3]. Since Cd and Bi have low melting points and the activities of Pu and the MAs in their liquid metal phases are very low [6], Cd and Bi are useful as typical liquid solvents for the reductive extraction method and liquid cathodes for the electrorefining method. Therefore, several studies have been conducted on the distribution behaviours of U, Pu and the MAs between the LiCl–KCl eutectic melt and liquid Cd or Bi, and the activities of these elements in liquid Cd or Bi phase [7–10]. The authors have reported the redox potentials of the U^{3+}/U and Pu^{3+}/Pu couples at the liquid Cd and Bi electrodes in LiCl–KCl melts by considering the formation energies of intermetallic compounds [11–13]. For Np, although the thermochemical information such as the formation energies of intermetallic compounds and the solubilities on Np in the liquid Cd and Bi phases has already been reported [14–16], the information on the electrode reaction of the Np^{3+}/Np couple at the liquid Cd and Bi electrodes has not yet been reported.

In the present study, the electrode reactions of the Np^{3+}/Np couple at the surface of the liquid Cd and Bi were investigated, then comparing them to that at a solid Mo electrode. The differences between the redox potential of the Np^{3+}/Np couple at the solid electrode and those at the liquid Cd and Bi electrodes were thermodynamically interpreted by the formation energies of the Np–Cd alloy and Np–Bi alloy.

2. Experimental details

The electrochemical cell used for the voltammetric studies was previously shown [11]. Liquid Cd and Bi

electrodes, used as the working electrodes, were prepared as follows. Some granules of Cd (99.999%; Soekawa Chemicals Co.) and of Bi (99.99%; Soekawa Chemicals Co.) were placed in separate crucibles made of high-purity aluminum nitride (99.6% AlN; Nikkato Co.). The crucibles were immersed in the LiCl–KCl melt phase. A Mo wire (>99.95%; Soekawa Chemicals Co.) of 1.0 mm diameter sheathed with a high purity alumina tube of 1.0 mm inner diameter and 2.0 mm outer diameter was then immersed in the liquid metal phase to be used as a lead wire. The surface area of the liquid metal electrode was 0.605 cm^2, ignoring the distortion of the liquid metal surface due to the surface tension and wetting of the surface of the crucible. Before every voltammetric scan, Np was released from the liquid Cd and Bi phases and into the salt phase by the application of −0.8 and −0.6 V, respectively, on the surface of the liquid Cd and Bi phases. A Mo wire of 1.0 mm diameter also served as a working electrode in order to compare it with the Cd and Bi electrodes. The Mo wire was encased in a high purity alumina tube in such a way that the apparent surface area of 0.332 cm^2 was exposed to the molten salt. A silver–silver chloride (Ag/AgCl) electrode served as the reference electrode. The reference electrode consisted of a closed-end porous mullite tube (50% Al_2O_3 + 46% SiO_2; Nikkato Co.), in which the LiCl–KCl eutectic salt containing 1.00 wt % AgCl was placed, and an Ag wire of 1.0 mm diameter was immersed in the salt. A carbon rod (99.998%; Tokai Carbon Co.) of 3.0 mm diameter sheathed with a high purity alumina tube of 3.0 mm inner diameter and 5.0 mm outer diameter was used as the counter electrode. The surface area of the carbon counter electrode in contact with the salt phase was about 6.5 cm^2. The temperature of the molten salt was controlled to ±0.5 K by a calibrated chromel–alumel thermocouple immersed in the electrolyte. Cyclic voltammograms were obtained using a voltammetric analyser (BAS CV-50W).

The polarographic-grade LiCl–KCl eutectic and $CdCl_2$ salts were obtained from the Anderson Physics Laboratory. By reacting $CdCl_2$ in the LiCl–KCl eutectic melt with Np in the molten Cd phase at 773 K, the salt phase containing about 20 wt % $NpCl_3$ was prepared [17]. This salt was added to the LiCl–KCl eutectic melt in order to adjust the concentration of $NpCl_3$ for the cyclic voltammetry. The concentration of $NpCl_3$ in the LiCl–KCl eutectic melts was determined by ICP–AES.

The voltammetric measurements were carried out in a glovebox with a high-purity argon gas atmosphere (H_2O, O_2 < 2.0 ppm).

3. Results and discussion

3.1. *Electrode reaction of the Np^{3+}/Np couple at the liquid Cd electrode*

Cyclic voltammograms for the redox reaction of the Np^{3+}/Np couple are shown in Figure 1. Curve 1 shows

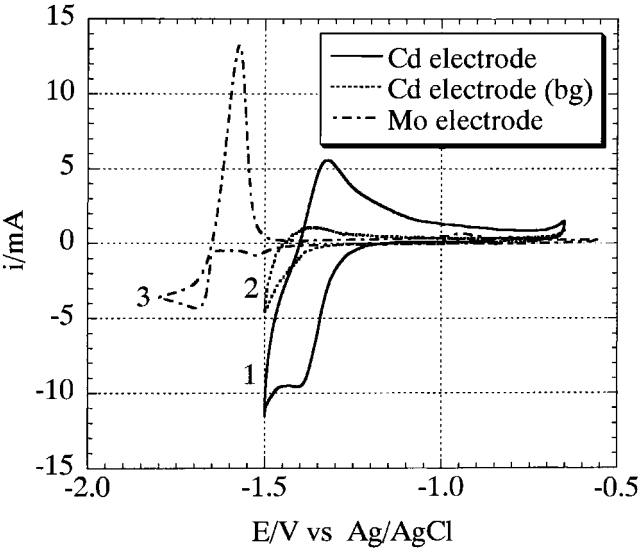

Fig. 1. Cyclic voltammograms for the redox reaction of the Np^{3+}/Np couple at the liquid Cd electrode (curves 1 and 2) and at the Mo electrode (curve 3) at 723 K. Scan = 0.01 V s^{-1}; concentration of $NpCl_3$ 0.465 wt % (curves 1 and 3), none (curve 2); apparent area of the working electrode 0.605 cm^2 (curves 1 and 2), 0.322 cm^2 (curve 3).

the voltammogram for the redox reaction at the interface between the LiCl–KCl eutectic melt containing 0.465 wt % (7.00×10^{-4} mole fraction) $NpCl_3$ and liquid Cd at a scan rate of 0.01 V s^{-1} at 723 K. Curve 2 shows the voltammogram obtained at the interface between the LiCl–KCl melt in the absence of $NpCl_3$ and liquid Cd. The final rise derived from the oxidation of Cd ($Cd = Cd^{2+} + 2e^-$) was observed when the potential of the liquid Cd electrode was scanned to potentials more positive than −0.6 V. The final descents observed around −1.5 V in curves 1 and 2 correspond to the reduction of Li^+ ($Li = Li^+ + e^-$); this was presumed from the relation between the redox potential of the Li^+/Li couple and the formation energy of the Li–Cd alloy [18]. Here, the final rise and the final descent involve large positive and negative currents, respectively, limiting the potential window. There are cathodic and anodic peaks in curve 1. In the region of potential scanning between 0.01 and 0.20 V s^{-1}, the anodic and the cathodic peak potentials, E_p^a and E_p^c, remained almost constant. These peaks may be attributed to the redox reaction of the Np^{3+}/Np couple, since the number of transferred electrons was calculated to be 2.8–2.9 from the relation between E_p^c and the cathodic half-peak potential, $E_{p/2}^c$, of the cyclic voltammograms obtained at 723 K in the region of the potential scanning rate between 0.01 to 0.20 V s^{-1} ($E_p^c - E_{p/2}^c = -2.2RT/nF$) [19]. Figure 2 shows that a plot of the cathodic peak current against the square root of the scan rate is approximately linear between 0.01 and 0.50 V s^{-1}. The cathodic peak current was proportional to the concentration of $NpCl_3$ and increased with temperature, as shown in Figure 3. The temperature dependence of the peak current can be understood by considering the

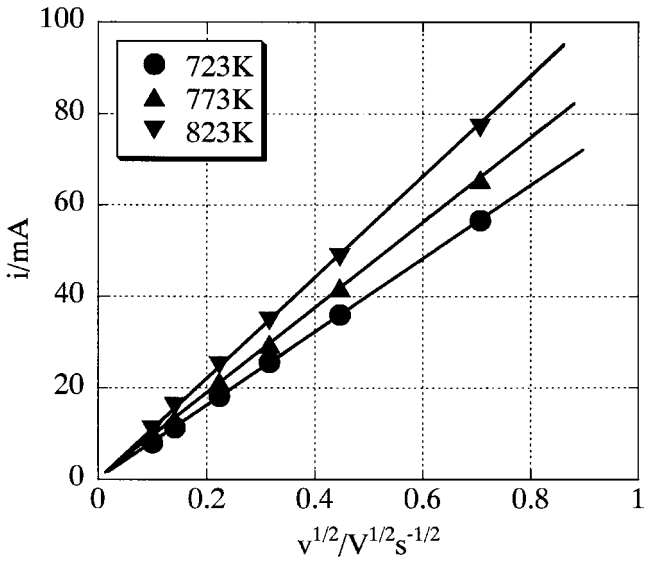

Fig. 2. Plot of cathodic peak current against square root of the potential scanning rate (v) on the cyclic voltammograms for the redox reaction of the Np^{3+}/Np couple at the Cd electrode at 723 K. Concentration of $NpCl_3$ 0.465 wt %; apparent area of Cd electrode 0.605 cm^2.

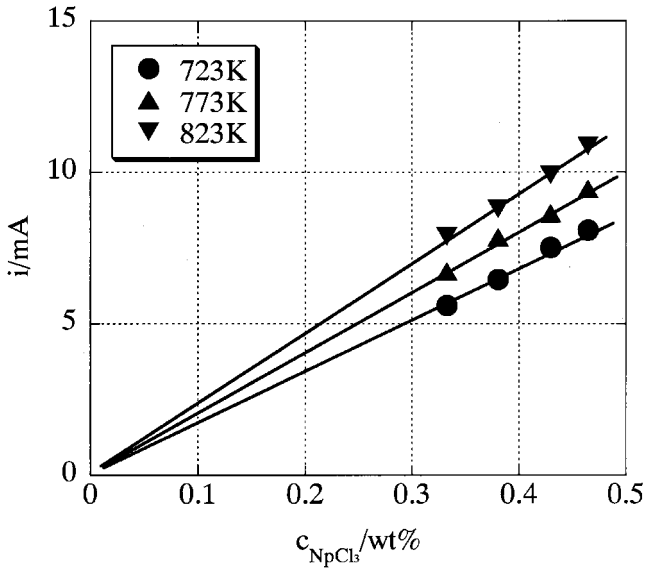

Fig. 3. Plot of cathodic peak current against concentration of $NpCl_3$ (c_{NpCl_3}) on the cyclic voltammograms for the redox reaction of the Np^{3+}/Np couple at Cd electrode at 723, 773 and 823 K. Scan rate 0.01 V s^{-1}; apparent area of Cd electrode 0.605 cm^2.

temperature dependence of the diffusion coefficient of Np^{3+} in the salt {723 K; $(1.73 \pm 0.09) \times 10^{-5}$ cm^2 s^{-1}, 773 K; $(2.48 \pm 0.15) \times 10^{-5}$ cm^2 s^{-1}, 823 K; $(3.48 \pm 0.23) \times 10^{-5}$ cm^2 s^{-1}} [17]. The above characteristics indicate that the redox reaction of the Np^{3+}/Np couple is almost reversible under the experimental conditions. The redox potential can be evaluated from the half wave potential, $E_{1/2}$, which is approximated by the midpoint potential, E_m, between E_p^c and E_p^a [20]. The $E_{1/2}$ values at 723, 773 and 823 K are -1.361 ± 0.002 V, -1.345 ± 0.002 and -1.321 ± 0.002 V, respectively, as shown in Table 1. On the other hand, $E_{1/2}$ values can also be estimated from the relation between $E_{1/2}$ and E_p^c, -1.364 ± 0.002 V, -1.345 ± 0.002 and -1.322 ± 0.002 V at 723, 773 and 823 K, respectively, and that between $E_{1/2}$ and $E_{p/2}^c$, -1.362 ± 0.002 V, -1.344 ± 0.002 and -1.321 ± 0.002 V at 723, 773 and 823 K, respectively. These values are in fair agreement with the E_m values.

The cathodic and anodic peaks correspond to the redox reaction of the Np^{3+}/Np couple in the case of a Mo working electrode in the $NpCl_3$–LiCl–KCl system, as shown by curve 3 in Figure 1 [17]. Table 2 shows that the redox potentials of the Np^{3+}/Np couple at the liquid Cd electrode at 723, 773 and 823 K appeared more positively by about 0.158, 0.140 and 0.126 V, respectively, than those at the Mo electrode. It was postulated that the potential difference between the redox potentials of the Np^{3+}/Np couple at the liquid Cd electrode and those at the Mo electrode were attributed to a lowering of the activity of Np in the Cd phase [6,15], from the analogy to other cases such as the electrode reaction of the Pu^{3+}/Pu couple at the liquid Cd electrode [11]. Since activitiy of Np in the Cd phase depends on the dissolved condition and concentration of Np in the Cd phase, the potential difference can be explained as described below by assuming the formation of the $NpCd_n$ ($n = 6$, 11) alloy which is a stable intermetallic compound among the Np–Cd system. $NpCd_n$ will be formed in the liquid Cd phase according to Equation 1.

$$Np + nCd = NpCd_n \tag{1}$$

The thermodynamic equilibrium constant, K_{NpCd_n}, in the above reaction is written as Equation 2:

$$K_{NpCd_n} = [NpCd_n]_{Cd} / \{[Np]_{Cd}[Cd]_{Cd}^n\} \tag{2}$$

where the square brackets, $[\ ]_{Cd}$, represent the activities of $NpCd_n$, Np and Cd in the liquid Cd phase, respectively. On the other hand, the redox potential of the Np^{3+}/Np couple at the solid electrode *vs* the Ag/AgCl reference electrode, $E_{Np^{3+}/Np}$, is expressed as follows:

$$E_{Np^{3+}/Np} = E^{\circ\prime}_{Np^{3+}/Np} + \frac{RT}{3F} \ln\left[\frac{[Np^{3+}]}{[Np]}\right] \tag{3}$$

Here, $E^{\circ\prime}_{Np^{3+}/Np}$ is the formal potential and T is the temperature in K. Accordingly, the redox potential of the Np^{3+}/Np couple at the liquid Cd electrode, $E_{Np^{3+}/Np-Cd}$, is described by considering Equations 2 and 3 as follows:

$$E_{Np^{3+}/Np-Cd} = E^{\circ\prime}_{Np^{3+}/Np} + \frac{RT}{3F} \ln\left[\frac{K_{NpCd_n}[Np^{3+}][Cd]_{Cd}^n}{[NpCd_n]_{Cd}}\right] \tag{4}$$

Equation 4 can be transformed into Equation 5.

Table 1. Cathodic and anodic peak potentials, E_p^c and E_p^a, and cathodic half-peak potential, $E_{p/2}^c$, in the cyclic voltammograms for the redox reaction of the Np^{3+}/Np couple at liquid Cd electrode in the LiCl–KCl eutectic melt containing 0.333, 0.380, 0.430 and 0.465 wt % $NpCl_3$ at 723, 773 and 823 K

$NpCl_3$ conc. /wt %	Temperature /K	E_p^c /V	E_p^a /V	E_m /V	$E_{p/2}^c$ /V
	723	−1.388	−1.336	−1.362	−1.339
0.333	773	−1.371	−1.318	−1.345	−1.321
	823	−1.348	−1.294	−1.321	−1.296
	723	−1.387	−1.334	−1.361	−1.338
0.381	773	−1.369	−1.317	−1.343	−1.318
	823	−1.346	−1.291	−1.319	−1.293
	723	−1.389	−1.335	−1.362	−1.341
0.430	773	−1.372	−1318	−1.345	−1.321
	823	−1.348	−1.293	−1.321	−1.295
	723	−1.386	−1.334	−1.360	−1.337
0.465	773	−1.371	−1.319	−1.345	−1.321
	823	−1.349	−1.293	−1.321	−1.296

Table 2. Standard redox potentials of the Np^{3+}/Np couple in the LiCl–KCl eutectic melt containing $NpCl_3$ ($E^{\circ\prime}_{Np^{3+}/Np}$) [17], those at Cd electrode ($E^{\circ\prime}_{Np^{3+}/Np-Cd}$), potential differences (ΔE) between $E^{\circ\prime}_{Np^{3+}/Np}$ and $E^{\circ\prime}_{Np^{3+}/Np-Cd}$, free energies of formation of $NpCd_x$ in Cd phase (ΔG) estimated from ΔE values, free energies of formation of $NpCd_6$ ($\Delta G^\circ_{fNpCd_6}$) [6] and free energies of formation of $NpCd_{11}$ ($\Delta G^\circ_{fNpCd_{11}}$) [6]

Temp. /K	$E^{\circ\prime}_{Np^{3+}/Np}$ /V	$E^{\circ\prime}_{Np^{3+}/Np-Cd}$ /V	ΔE /V	ΔG /kJ mol^{-1}	$\Delta G^\circ_{fNpCd_6}$ /kJ mol^{-1}	$\Delta G^\circ_{fNpCd_{11}}$ /kJ mol^{-1}
723	−1.5191	−1.361	0.158	45.7	55.4	58.9
773	−1.4845	−1.345	0.140	40.5	51.3	50.8
823	−1.4474	−1.321	0.126	36.5	47.2	42.7

$$E_{Np^{3+}/Np-Cd} = E^{\circ\prime}_{Np^{3+}/Np} - \frac{\Delta G^\circ_{NpCd_n}}{3F} + \frac{RT}{3F}\ln[Np^{3+}] + \frac{nRT}{3F}\ln[Cd]_{Cd} - \frac{RT}{3F}\ln[NpCd_n]_{Cd} \quad (5)$$

where $\Delta G^\circ_{NpCd_n}$ is the standard Gibbs energy for the formation of $NpCd_n$ ($\Delta G^\circ_{NpCd_n} = -RT\ln K_{NpCd_n}$). Therefore, the potential difference, ΔE, between $E_{Np^{3+}/Np-Cd}$ and $E_{Np^{3+}/Np}$ is represented by Equation (6):

$$\Delta E = -\frac{\Delta G^\circ_{NpCd_n}}{3F} + \frac{nRT}{3F}\ln[Cd]_{Cd} - \frac{RT}{3F}\ln[NpCd_n]_{Cd} \quad (6)$$

Since solubilities of Np in the Cd phase, $[Np]_{Cd}$, at 723, 773 and 823 K are 0.011, 0.022 and 0.030 in mole fraction, respectively, most of the deposited Np should exist as solid $NpCd_{11}$ (650–758 K) or $NpCd_6$ (758–850 K) in the vicinity of the surface of the liquid Cd phase [6,15]. It seems reasonable to assume that $[NpCd_n]_{Cd}$ is locally close to unity. Taking into account the above assumptions, Equation 6 can be simplified to Equation 7:

$$\Delta E = -\frac{\Delta G^\circ_{NpCd_n}}{3F} + \frac{nRT}{3F}\ln[Cd]_{Cd} \quad (7)$$

$\Delta G^\circ_{NpCd_{11}}$ in the temperature region between 650 and 758 K and $\Delta G^\circ_{NpCd_6}$ in the temperature region between 758 and 850 K are given by the following equations, respectively [6,15]:

$$\Delta G^\circ_{NpCd_{11}} = -175900 + 161.8 \times T(\mathrm{J\,mol^{-1}}, 650 - 758\,\mathrm{K}), \quad (8)$$

$$\Delta G^\circ_{NpCd_6} = -115100 + 82.51 \times T(\mathrm{J\,mol^{-1}}, 758 - 850\,\mathrm{K}) \quad (9)$$

The following relation always holds between $[Cd]_{Cd}$ and the $[Np]_{Cd}$ in principle:

$$[Cd]_{Cd} + [Np]_{Cd} = 1 \quad (10)$$

Since the $[Np]_{Cd}$ values at 723, 773 and 823 K are regarded as the solubilities of Np in the liquid Cd phase at 723, 773 and 823 K, respectively, the $[Cd]_{Cd}$ values at 723, 773 and 823 K are calculated to be 0.989, 0.978 and 0.970, respectively. When Equations 8–10 are substituted in Equation 7, the ΔE values at 723, 773 and 823 K are estimated to be 0.201, 0.174 and 0.159 V, respectively. These values are 0.03–0.04 V greater than the experimental values. When the potential differences between the redox potentials of the Np^{3+}/Np couple at the Mo electrode and those at the liquid Cd electrode are transformed into Gibbs free energies, the variation in the free energies with temperature is similar to that

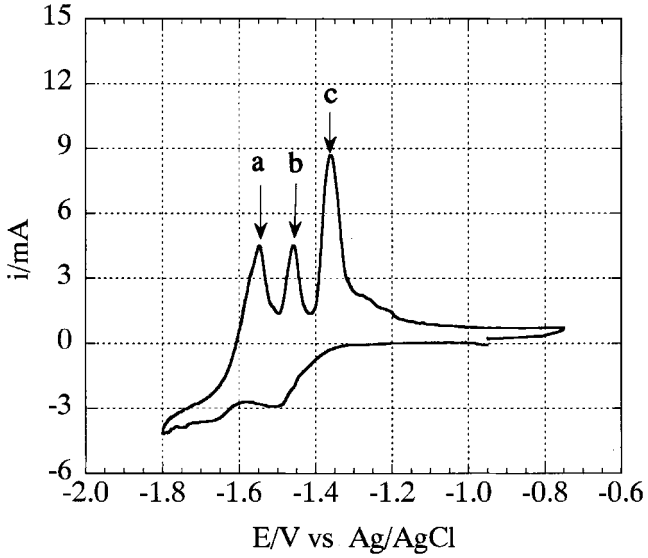

Fig. 4. Cyclic voltammograms for the redox of the Np^{3+}/Np couple at the Cd-coated Mo electrode at 723 K. Concentration of $NpCl_3$ 0.465 wt %; apparent area of Cd-coated Mo electrode 0.322 cm^2.

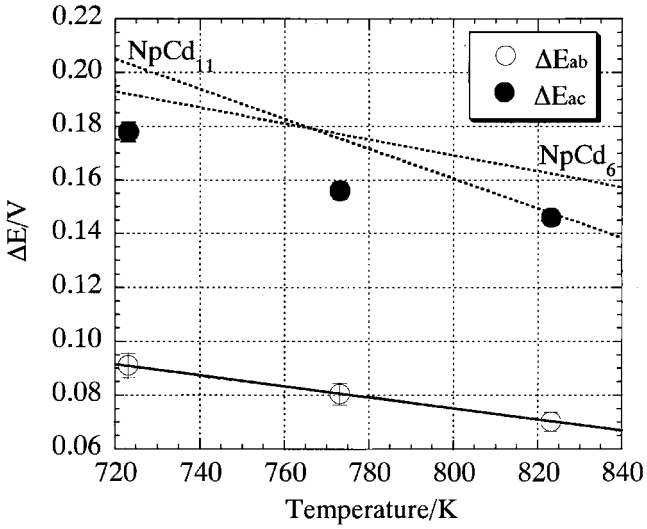

Fig. 5. Plots of potential difference between peaks **a** and **b** (ΔE_{ab}) against temperature (○) and that between peaks **a** and **c** (ΔE_{ac}) (●). Concentration of $NpCl_3$ in the salt 0.465 wt %.

evaluated using Equations 8 and 9 as noted in Table 2. This result suggests that the potential shift almost corresponds to the Gibbs free energy for the formation of the intermetallic compound, $NpCd_n$, in the liquid the Cd phase.

3.2. *Electrode reaction of the Np^{3+}/Np couple at the Cd-coated Mo electrode*

In order to investigate the effect of the alloy formation on the electrode reaction, the Cd-coated Mo electrode, which was prepared by the electrodeposition of Cd (~0.01 C) on the surface of the Mo electrode, was used as the working electrode. The solid line in Figure 4 shows a cyclic voltammogram for the redox of the Np^{3+}/Np couple at the Cd-coated Mo electrode. The experimental conditions were identical to those for curve 3 in Figure 1. There are several cathodic and anodic peaks in the voltammogram. The characteristics of the anodic peaks, **a**–**c**, are discussed hereafter, since the cathodic peaks due to the formation of the intermetallic compounds such as $NpCd_{11}$ and $NpCd_6$ were not clear in the voltammogram. The anodic peak **a** is considered to correspond to the dissolution of the Np metal based on the comparison with curve 3 in Figure 1. The potential difference between **a** and **b**, ΔE_{ab}, and that between **a** and **c**, ΔE_{ac}, are compared in Figure 5 as a function of temperature. The temperature dependence of ΔE_{ac} is almost identical to that of ΔE experimentally obtained as noted in the previous section, but the ΔE_{ac} values, which were 0.178 ± 0.005, 0.156 ± 0.005 and 0.146 ± 0.005, respectively, at 723, 773 and 823 K are 0.10–0.15 V greater than the ΔE values evaluated from the measurement of the electromotive force. Although the ΔE_{ac} values at 723, 773 and 823 K are 0.02–0.03 V less than the ΔE values estimated using Equations 7–9, the temperature dependence of the ΔE_{ac} values also agrees with that of the estimated values. It is postulated that peak **c** results from the sum of the oxidation of $NpCd_6$ to $NpCd_{11}$ ($11\ NpCd_6 = 6\ NpCd_{11} + 5Np^+ + 15e^-$) and the following decomposition of $NpCd_{11}$ ($NpCd_{11} = 11Cd + Np^+ + 3e^-$) at 723 K or the decomposition of $NpCd_6$ ($NpCd_6 = 6Cd + Np^+ + 3e^-$) at 773 and 823 K.

For anodic peak **b**, the following relations are derived from the temperature dependence of the ΔE_{ab} values (in V).

$$\Delta E_{ab} = 0.235 - 0.00020 \times T \qquad (11)$$

The potential difference, ΔE_{ab}, is transformed into the Gibbs formation energy (in J mol^{-1}), ΔG_{ab}, as follows:

$$\Delta G_{ab} = -68000 + 58 \times T \qquad (12)$$

The appearance of the anodic peak **b** indicates the existence of $NpCd_4$ or $NpCd_2$, other than $NpCd_{11}$ and $NpCd_6$, is inferred from the analogy with the phase diagram between Cd and Pu [6, 21]. During the voltammetric measurement, the amount of Cd adsorbed on the Mo electrode is constant. For one Cd atom in each reaction, the numbers of electrons involved in the decomposition of $NpCd_4$ ($3NpCd_4 = 2NpCd_6 + Np^+ + 3e^-$), that of $NpCd_2$ ($3NpCd_2 = NpCd_6 + 2Np^+ + 6e^-$) and that of the anodic reaction at peak **c** are 0.25, 2 and 0.5, respectively. Since the accumulated coulomb number of peak **b** is almost equal to half that of peak **c**, $NpCd_4$ is expected to be formed at the the Cd-coated Mo electrode.

In the case of the Cd-coated Mo electrode, the above results indicate that the analysis of the electrode reaction at the liquid metal-coated solid electrode would be available for the confirmation of the formation of

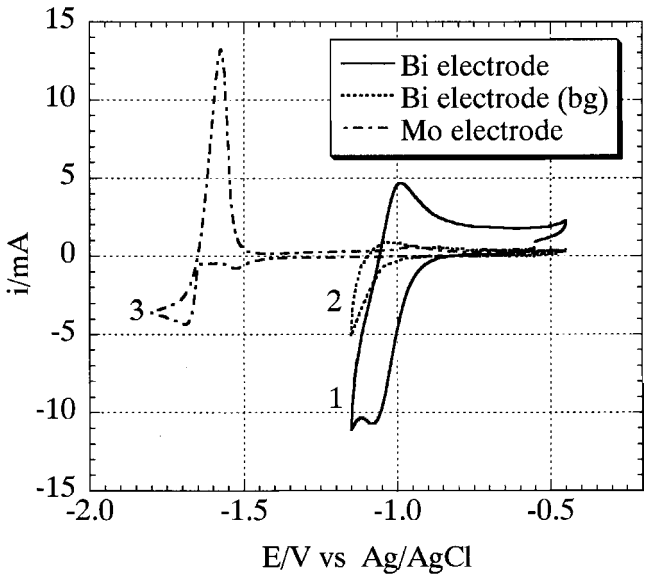

Fig. 6. Cyclic voltammograms for the redox reaction of the Np^{3+}/Np couple at the liquid Bi electrode (curves 1 and 2) and at the Mo electrode (curve 3) at 723 K. Scan = 0.01 V s^{-1}; concentration of $NpCl_3$ 0.465 wt % (curves 1 and 3), none (curve 2); apparent area of working electrode 0.605 cm^2 (curves 1 and 2), 0.322 cm^2 (curve 3).

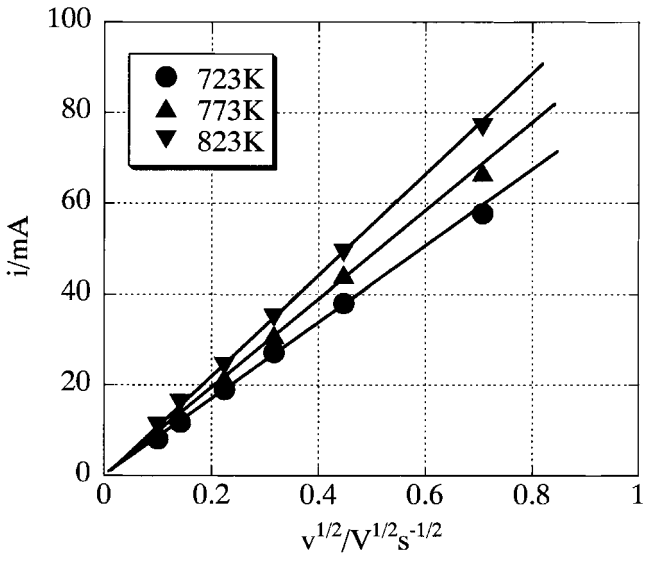

Fig. 7. Plot of cathodic peak current against square root of the potential scanning rate (v) on the cyclic voltammograms for the redox reaction of the Np^{3+}/Np couple at the Bi electrode at 723 K. Concentration of $NpCl_3$ 0.465 wt %; apparent area of Bi electrode 0.605 cm^2.

stoichiometric intermetallic compounds in the liquid metal electrode.

3.3. *Electrode reaction of the Np^{3+}/Np couple at the liquid Bi electrode*

Curve 1 in Figure 6 shows the voltammogram for the redox reaction of the Np^{3+}/Np couple in the LiCl–KCl eutectic melt containing 0.465 wt % $NpCl_3$ at the liquid Bi electrode at a scan rate of 0.01 V s^{-1} at 723 K. Curve 2 is the voltammogram obtained under the same condition but in the absence of $NpCl_3$. The large cathodic currents observed around −1.2 V in curves 1 and 2 must be attributable to the reduction of Li^+ to Li. There are cathodic and anodic peaks, which result from the redox reaction of the Np^{3+}/Np couple, in curve 1. In the region of the potential scanning rate between 0.01 and 0.20 V s^{-1}, E_p^a and E_p^c remained almost constant. These peaks must be attributed to the redox reaction of the Np^{3+}/Np couple, since the number of transferred electrons was calculated to be 2.9 ± 0.1 from the relation between E_p^c and $E_{p/2}^c$ in the cyclic voltammograms obtained at 723, 773 and 823 K in the region of the potential scanning rate between 0.01 to 0.20 V s^{-1}. Figure 7 shows that a plot of the cathodic peak current against the square root of the potential scanning rate is approximately linear between 0.01 and 0.50 V s^{-1}. The cathodic peak current was proportional to the concentration of $NpCl_3$ and increased with temperature, as shown in Figure 8. In the same manner as the redox reaction of the Np^{3+}/Np couple at the liquid Cd electrode, the temperature dependence of the peak current can be understood by considering the temperature dependence of the diffusion coefficient of Np^{3+} in

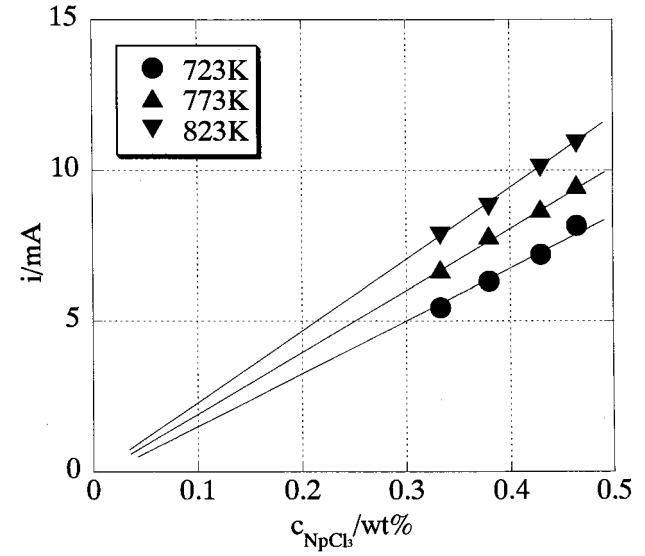

Fig. 8. Plot of cathodic peak current against the concentration of $NpCl_3$ (c_{NpCl_3}) on the cyclic voltammograms for the redox reaction of the Np^{3+}/Np couple at the Bi electrode at 723, 773 and 823 K. Scan rate 0.01 V s^{-1}; apparent area of Bi electrode 0.605 cm^2.

the salt. The above characteristics indicate that the redox reaction of the Np^{3+}/Np couple at the liquid Bi electrode is also reversible under the stated experimental conditions. By considering the relation between $E_{1/2}$ and E_p^c and that between $E_{1/2}$ and $E_{p/2}^c$, the $E_{1/2}$ values are estimated to be −1.092 ± 0.002 V, −1.066 ± 0.005 and −1.037 ± 0.010 V at 723, 773 and 823 K, respectively, as shown in Table 3.

The redox potentials of the Np^{3+}/Np couple at the liquid Bi electrode at 723, 773 and 823 K appeared more positive by about 0.427, 0.419 and 0.410 V, respectively,

Table 3. Cathodic and anodic peak potentials, E_p^c and E_p^a, mid-point potential, E_m, and cathodic half-peak potential, $E_{p/2}^c$, in the cyclic voltammograms for the redox reaction of the Np^{3+}/Np couple at liquid Bi electrode in the LiCl–KCl eutectic melt containing 0.333, 0.380, 0.430 and 0.465 wt % $NpCl_3$ at 723, 773 and 823 K

$NpCl_3$ conc. /wt %	Temp. /K	E_p^c /V	E_p^a /V	E_m /V	$E_{p/2}^c$ /V
	723	−1.117	−1.064	−1.091	−1.070
0.333	773	−1.091	−1.040	−1.066	−1.041
	823	−1.065	−1.008	−1.037	−1.010
	723	−1.119	−1.067	−1.093	−1.071
0.380	773	−1.094	−1.042	−1.068	−1.044
	823	−1.066	−1.005	−1.036	−1.009
	723	−1.119	−1.067	−1.093	−1.071
0.430	773	−1.090	−1.039	−1.065	−1.042
	823	−1.063	−1.007	−1.035	−1.009
	723	−1.117	−1.065	−1.091	−1.070
0.465	773	−1.092	−1.040	−1.066	−1.041
	823	−1.067	−1.007	−1.037	−1.010

Table 4. Standard redox potentials of the Np^{3+}/Np couple in the LiCl–KCl eutectic melt containing $NpCl_3$ ($E^{\circ\prime}_{Np^{3+}/Np}$) [17], those at the Bi electrode ($E^{\circ\prime}_{Np^{3+}/Np-Bi}$), potential differences (ΔE) between $E^{\circ\prime}_{Np^{3+}/Np}$ and $E^{\circ\prime}_{Np^{3+}/Np-Bi}$, free energies of formation of $NpBi_x$ estimated from ΔE values into the free energies (ΔG), and free energies for formation of $NpBi_2$ (ΔG_{fNpBi_2}) [16]

Temp. /K	$E^{\circ\prime}_{Np^{3+}/Np}$ /V	$E^{\circ\prime}_{Np^{3+}/Np-Bi}$ /V	ΔE /V	ΔG /kJ mol^{-1}	$\Delta G^{\circ}_{fNpBi_2}$ /kJ mol^{-1}
723	−1.5191	−1.092	−0.427	−123	−114.1
773	−1.4845	−1.066	−0.419	−121	−112.6
823	−1.4474	−1.037	−0.410	−119	−111.1

than those at the Mo electrode obtained from the measurement of the electromotive force [17]. Analogous to the electrode reaction for the Np^{3+}/Np couple at the liquid Cd electrode, the difference between the redox potentials of the Np^{3+}/Np couple at the liquid Bi electrode and those at the Mo electrode must be attributed to the lowering of the activity of Np in the Bi phase. Therefore, the potential difference can be explained as below by assuming the formation of $NpBi_2$ which is the most stable intermetallic compound in the Np–Bi system. $NpBi_2$ will be formed in the liquid Bi phase as Equation 13 [16]:

$$Np + 2Bi = NpBi_2 \tag{13}$$

Thus, analogous with the electrode reaction of the Np^{3+}/Np couple at the liquid Cd electrode, the redox potential of the Np^{3+}/Np couple at the liquid Bi electrode, $E_{Np^{3+}/Np-Bi}$, is described as follows:

$$E_{Np^{3+}/Np-Bi} = E^{\circ\prime}_{Np^{3+}/Np} + \frac{RT}{3F}\ln\frac{K_{NpBi_2}[Np^{3+}][Bi]^2_{Bi}}{[NpBi_2]_{Bi}} \tag{14}$$

where K_{NpBi_2} is the stability constant of $NpBi_2$. The potential difference, ΔE, between $E_{Np^{3+}/Np-Bi}$ and $E_{Np^{3+}/Np}$ is then represented as Equation 15.

$$\Delta E = -\frac{\Delta G^{\circ}_{NpBi_2}}{3F} + \frac{2RT}{3F}\ln[Bi]_{Bi} \tag{15}$$

The standard formation energy of $NpBi_2$, $\Delta G^{\circ}_{NpBi_2}$, in the temperature region between 673 and 773 K is given by the following equation [16]:

$$\Delta G^{\circ}_{NpBi_2} = -136000 + 30.12 \times T(\mathrm{J\,mol^{-1}}) \tag{16}$$

Since the solubilities of Np in the liquid Bi phase at 723, 773 and 823 K are 0.0061, 0.0106 and 0.0166, respectively, the minimum $[Bi]_{Bi}$ values at 723, 773 and 823 K are calculated to be 0.9939, 0.9894 and 0.9834, respectively, based on the following relation:

$$[Bi]_{Bi} + [Np]_{Bi} = 1 \tag{17}$$

When the $\Delta G^{\circ}_{NpBi_2}$ values and solubilities are substituted in Equation 15, the ΔE values at 723, 773 and 823 K are estimated to be 0.3946, 0.3894 and 0.3842 V, respectively, as noted in Table 4. Although these values are about 0.03 V lower than the experimental values previous mentioned, the temperature dependence of the ΔE values agrees with that of the reported values. When the potential differences between the redox reaction of the Np^{3+}/Np at the Mo electrode and that at the liquid Bi electrode are transformed into Gibbs free energies, the free energies almost agree with the values evaluated

using Equation 16. This result suggests that the potential shift almost corresponds to the Gibbs free energy for the formation of the intermetallic compound, $NpBi_2$, in the liquid Bi phase, analogous to the positive shift in potential when the liquid Cd electrode was used as a cathode.

4. Conclusion

The electrode reactions of the Np^{3+}/Np couple at the liquid Cd and Bi electrodes were elucidated by voltammetry. The redox reactions of the Np^{3+}/Np couple at the liquid Cd and Bi electrodes were almost reversible. This is probably due to the dispersion of the Np–Cd and Np–Bi alloys from the interface to the inner phase of the liquid Cd and Bi electrodes, respectively, though Np metal was deposited as Np–Cd and Np–Bi alloys at the surface of the liquid electrodes during the reduction of Np^{3+}. The depositon of Np at the liquid Cd and Bi electrodes were observed at potentials more positive by about 0.14 and 0.42 V than that at the Mo electrode. The potential shifts almost corresponded to the Gibbs free energies of formation for $NpCd_{11}$ (723 K) and $NpCd_6$ (773 and 823 K) in the liquid Cd phase and those for $NpBi_2$ (723, 773 and 823 K) in the liquid Bi phase.

Acknowledgements

The authors thank Mr. K. Shiozawa of JAERI for the ICP–AES analysis. We are grateful to Dr T. Inoue of CRIEPI, and Drs K. Iwamura and Z. Yoshida of JAERI for their interest and useful suggestions.

References

1. Y.I. Chang, *Nucl. Technol.* **88** (1989) 129.
2. J.P. Ackerman, *Ind. Eng. Chem. Res.* **30** (1991) 141.
3. M. Iizuka, T. Koyama, N. Kondo, R. Fujita and H. Tanaka, *J. Nucl. Mater.* **247** (1997) 183.
4. Y. Arai, T. Iwai, K. Nakajima and Y. Suzuki, Proceedings of the International Conference on 'Future Nuclear Systems' (GLOBAL'97), Vol. 1, Yokohama, Japan, 5–10, Oct. 1997, (1997), p. 664.
5. T. Ogawa, M. Akabori, Y. Suzuki, F. Kobayashi, T. Osugi and T. Mukaiyama, Proceedings, vol. 1, ref. [4], p. 812.
6. P. Chiotti, V.V. Akhachinskij, I. Ansara and M.H. Rand, *in* V. Medvedev et al. (Eds), The Chemical Thermodynamics of Actinide Elements and Compounds, Part 5 The Actinide Binary Alloys (International Atomic Energy Agency, Vienna, 1981).
7. J.P. Ackerman and J.L. Settle, *J. Alloys Comp.*, 199 (1993) 77.
8. T. Koyama, T.R. Johnson and D.F. Fischer, *J. Alloys Comp.* **189** (1992) 37.
9. M. Kurata, Y. Sakamura, T. Hijikata and K. Kinoshita, *J. Nucl. Mater.* **227** (1995) 110.
10. H. Moriyama, H. Yamana, S. Nishikawa, S. Shibata, N. Wakayama, Y. Miyashita, K. Moritani and T. Mitsugashira, *J. Alloys Comp.* **271–273** (1998) 587.
11. O. Shirai, M. Iizuka, T. Iwai, Y. Suzuki and Y. Arai, *J. Electroanal. Chem.* **490** (2000) 31.
12. O. Shirai, M. Iizuka, T. Iwai, Y. Suzuki and Y. Arai, *Anal. Sci.* **17** (2001) 51.
13. O. Shirai, K. Uozumi, T. Iwai and Y. Arai, *Anal. Sci.* **17** (2002) i959.
14. M. Krumpelt, I. Johnson and J.J. Heiberger, *J. Less-Common Metals* **18** (1969) 35.
15. M. Krumpelt, I. Johnson and J.J. Heiberger, *Metall. Trans.* **5** (1974) 65.
16. Y. Sakamura, O. Shirai, T. Iwai and Y. Arai, *J. Electrochem. Soc.* **147** (2000) 642.
17. O. Shirai, M. Iizuka, T. Iwai and Y. Arai, *J. Appl. Electrochem.* **31** (2001) 1055.
18. M.A. Lewis and T.R. Johnson, *J. Electrochem. Soc.* **137** (1990) 1414.
19. A.J. Bard and L.R. Faulkner, 'Electrochemical Methods: Fundamentals and Applications' (John Wiley & Sons, New York 1980), chapter 6.
20. D.K. Gosser, Jr, 'Cyclic Voltammetry: Simulation and Analysis of Reaction Mechanisms' (VCH, New York, 1993), chapter 2.
21. I. Johnson, M.G. Chasanov and R.M. Yonco, *Trans. Met. Soc. AIME* **233** (1965) 1408.